# Facile and fast determination of Si/Al ratio of zeolites using FTIR spectroscopy technique

Yik-Ken Ma, Severinne Rigolet, Laure Michelin, Jean-Louis Paillaud, Svetlana Mintova, Fitri Khoerunnisa, T. Jean Daou, Eng-Poh Ng

# Facile and fast determination of Si/Al ratio of zeolites using FTIR spectroscopy technique

Yik-Ken Ma[a], Severinne Rigolet[b,c], Laure Michelin[b,c], Jean-Louis Paillaud[b,c], Svetlana Mintova[d], Fitri Khoerunnisa[e], T. Jean Daou[b,c,**], Eng-Poh Ng[a,*]

[a] School of Chemical Sciences, Universiti Sains Malaysia, 11800, USM, Penang, Malaysia
[b] Université de Haute-Alsace, Axe Matériaux à Porosité Contrôlée, Institut de Science des Matériaux de Mulhouse UMR 7361, ENSCMu, 3bis Rue Alfred Werner, 68093, Mulhouse, France
[c] Université de Strasbourg, 67000, Strasbourg, France
[d] Laboratoire Catalyse & Spectrochimie, ENSICAEN, Université de Caen, 14000, Caen, France
[e] Chemistry Education Department, Universitas Pendidikan Indonesia, Jl. Setiabudhi 258, Bandung, 40514, Indonesia

* Corresponding author.
** Corresponding author. Université de Haute-Alsace, Axe Matériaux à Porosité Controlée, Institut de Science des Matériaux de Mulhouse UMR 7361, ENSCMu, 3bis rue Alfred Werner, 68093, Mulhouse, France.
*E-mail addresses:* jean.daou@uha.fr (T.J. Daou), epng@usm.my (E.-P. Ng).

**To cite this article:** Facile and fast determination of Si/Al ratio of zeolites using FTIR spectroscopy technique, Microporous Mesoporous Mater., 2021, 311, 110683. DOI : 10.1016/j.micromeso.2020.110683, HAL : hal-02968402.
Received 12 August 2020; Received in revised form 25 September 2020; Accepted 6 October 2020, Available online 9 October 2020

*Keywords:* Infrared spectroscopy ; Zeolites ; Si/Al ratio ; Vibration bands ; Quantitative analysis

**ABSTRACT:** A facile quantitative determination of the Si/Al ratio (SAR) in zeolite frameworks using IR spectroscopy is re- ported. From the linear regression analysis, the SAR for the medium-to-high Al content zeolites (1 < SAR < 5) correlates linearly to the corresponding intensity of the IR band at wavenumbers (950-1090 $cm^{-1}$). This model has been validated with 19 zeolites with different SAR and different framework topologies (EDI, ABW, EMT, MER, LTL, LTJ, MOR, FAU, SOD, HEU, BRE, OFF, GIS, *BEA, MFI). The quantitative determination of the SAR of zeolites by IR spectroscopy is shown to be an alternative technique to the conventional ICP-OES and XRF spectroscopy techniques.

## 1. Introduction

Zeolites are very important and useful industrial materials used in adsorption, separation and catalysis due to their various micropore sizes and unique framework properties [1–3]. Besides the structural proper- ties, the Al content in the framework or so-called Si/Al ratio (SAR) is of great importance and governs their applications [4,5].

In general, the most common analytical techniques for the identifi- cation of Al content in zeolites are X-ray fluorescence spectroscopy (XRF), atomic absorption spectroscopy (AAS), inductively coupled plasma atomic emission spectroscopy (ICP-OES), X-ray diffraction (XRD) and solid state Si nuclear magnetic resonance spectroscopy ( Si NMR). However, these analytical tools face some limitations particularly in sample preparation workout, measurement time dura- tion, post-analytical interpretation treatment, etc. (Table 1). Therefore, the development of fast, simple and reliable method for quantitatively determining the SAR in the zeolite framework is highly desired.

Fourier-transform infrared spectroscopy (IR) is often used to study zeolites with emphasis on the functional groups, structural features, secondary building units (SBUs), pore openings and surface particular- ities. In the mid IR region (200–1300 cm ), the vibrations associated with the framework structure are presented. In past few decades, several reports dealing with the use of IR spectroscopy for evaluation of zeolite particularities were published. The pioneer and iconic work was re- ported by Flanigen et al. [6]. Other studies presenting detailed and systematic spectroscopy studies on various aluminosilicate zeolites were also published [7–9]. They found out that the positions of certain IR bands at 970-1020 $cm^{-1}$, 670-725 $cm^{-1}$, 565-580 $cm^{-1}$ and 360-385 $cm^{-1}$ have a linearity with the Al content in faujasite type zeolites [7]. Since then, Lohse et al. reported on the use of the IR band at 748-837 $cm^{-1}$ to calculate the SAR of cubic and hexagonal faujasite zeolites [8]. However, the validity of IR spectroscopy method for identifying the SAR is only limited to faujasites. Hence, the development of theoretical cal- culations using IR spectroscopy to determine the SAR in various zeolite frameworks is still not yet developed and remains unclear.

In this communication, we present the IR spectroscopy protocol to- wards the determination of the SAR of zeolites; this protocol was developed based on 19 zeolites subjected to comprehensive characterization with the classical chemical analyses (ICP and XRF) and NMR spectroscopy technique.

**Table 1**
Advantages (✓) and disadvantages ( × ) of various spectroscopy techniques used for determination of the SAR of zeolites.

| | ICP-OES | AAS | XRF | XRD | IR | $^{29}$Si NMR |
|---|---|---|---|---|---|---|
| Sample recovery | × | × | ✓ | ✓ | ✓ | ✓ |
| Fast analysis | × | × | × | × | ✓ | × |
| Small sample quantity required | ✓ | ✓ | × | × | ✓ | × |
| Simple sample preparation | × | × | ✓ | ✓ | ✓ | ✓ |
| Post-treatment requirement | × | × | × | ✓ | × | ✓ |

## 2. Experimental

### *2.1. Analytical procedures*

19 types of zeolites with various framework topologies and SAR ratios were selected and synthesized according to the procedures reported previously [10–25] (See Supplementary Information). The FTIR spectra of the zeolites were recorded with a Perkin Elmer's System 2000 IR spectrometer (1400-400 cm$^{-1}$, resolution of 2 cm$^{-1}$, 100 scans) using the KBr pellet technique. The chemical composition of samples was determined using a Varian Vista MPX ICP-OES and XGT-5200 XRF spectrometers. For ICP-OES spectroscopy analysis, the zeolite powder (0.0005 g) was first dissolved in HF solution (2 mL, 39%, Merck) for at least 12 h under stirring before dilution and filtration using 0.45-μm microfilter. Boric acid was added to minimize fluoride interferences during measurement. For Si MAS NMR spectroscopy measurement, the analysis was performed with a Bruker Avance II 300 MHz spectrometer according to the procedure reported previously [26] and the Si/Al ratio was calculated using the Engelhard's equation [27]:

$$Si/Al = \frac{\sum_{n=0}^{4} I_{Si(nAl)}}{\sum_{n=0}^{4} (n/4) I_{Si(nAl)}} \qquad (1)$$

where n is the number of adjacent Al nuclei, I is the relative intensity of each $^{29}$Si NMR signals ($Q^0$–$Q^4$).

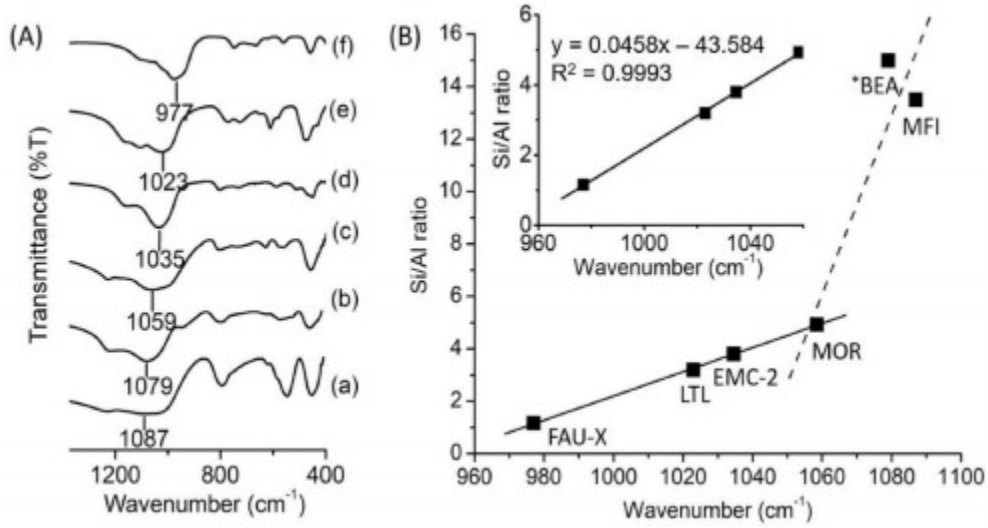


**Fig. 1.** (A) IR spectra of (a) Na-ZSM-5 (SAR = 13.5), (b) Na-Beta (SAR = 15.1), (c) Na-mordenite (SAR = 4.93), (d) Na-EMC-2 (SAR = 3.76), (e) K-L (SAR = 3.20) and (f) Na-X (SAR = 1.16) zeolites, and (B) the linear regression analysis of the SAR versus the position of asymmetric stretching Si–O–T(T = Si or Al) bands at 950-1090 cm$^{-1}$.

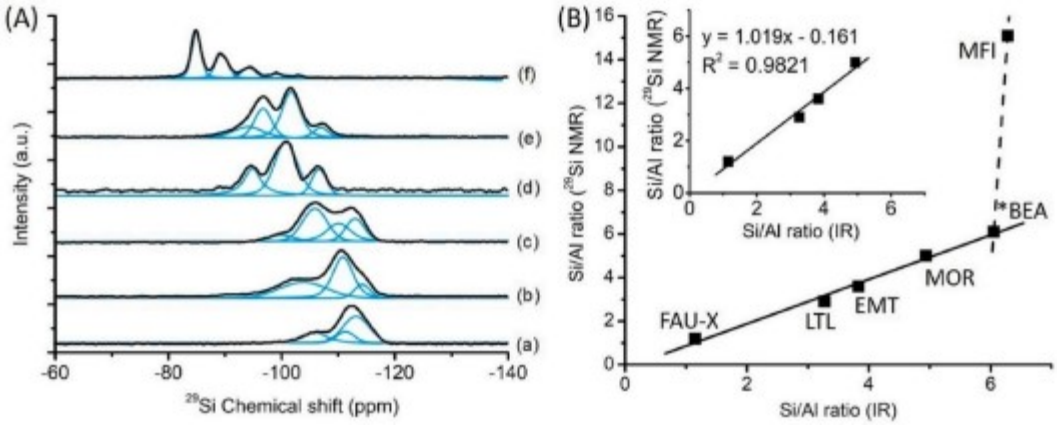


**Fig. 2.** (A) $^{29}$Si MAS NMR spectra of (a) Na-ZSM-5, (b) Na-Beta, (c) Na-mordenite, (d) Na-EMC-2, (e) K-L and (f) Na-X zeolites, and (B) the linear regression correlation of the SAR estimated by IR spectroscopy and $^{29}$Si MAS NMR spectroscopy.

**Table 2**
The positions corresponding asymmetric stretching Si–O-T (T = Si or Al) bands at 950-1090 cm$^{-1}$ ($x$) used for estimation of the SAR of zeolites ($y$) using linear regression equation: $y = 0.0458x - 43.584$, and the SAR values determined by ICP-OES and XRF spectroscopy.

| No. | Zeolites | Framework code | Wavenumber (cm$^{-1}$) | Si/Al ratio | | |
|---|---|---|---|---|---|---|
| | | | | IR[a] | ICP-OES | XRF |
| 1. | K-F | **EDI** | 973 | 0.98 | 1.26 | 1.02 |
| 2. | Cs-ABW | **ABW** | 985 | 1.53 | 1.03 | 1.13 |
| 3. | Na-EMT | **EMT** | 980 | 1.30 | 1.16 | 1.18 |
| 4. | K-W | **MER** | 992 | 1.85 | 2.30 | 2.19 |
| 5. | K-L | **LTL** | 1023 | 3.27 | 3.20 | 2.93 |
| 6. | K-J | **LTJ** | 987 | 1.62 | 1.86 | 1.77 |
| 7. | Na-Mordenite | **MOR** | 1059 | 4.92 | 4.93 | 4.88 |
| 8. | Na-X | **FAU** | 977 | 1.16 | 1.16 | 1.18 |
| 9. | Na-Y | **FAU** | 996 | 2.03 | 1.98 | 2.13 |
| 10. | Na-EMC-2 | **EMT** | 1035 | 3.82 | 3.76 | 3.71 |
| 11. | Hydroxysodalite | **SOD** | 983 | 1.44 | 1.10 | 1.14 |
| 12. | Na-A | **LTA** | 952 | 0.02 | 1.04 | 0.98 |
| 13. | Heulandite | **HEU** | 1026 | 3.41 | 3.50 | 3.48 |
| 14. | Brewsterite | **BRE** | 1012 | 2.77 | 3.00 | 2.91 |
| 15. | Na-LSX | **FAU** | 973 | 0.98 | 0.98 | 1.03 |
| 16. | Offretite | **OFF** | 1037 | 3.91 | 3.89 | 3.76 |
| 17. | Na-P | **GIS** | 983 | 1.44 | 1.35 | 1.44 |
| 18. | Na-BEA | ***BEA** | 1083 | 6.02 | 15.1 | 15.0 |
| 19. | Na-ZSM-5 | **MFI** | 1088 | 6.25 | 13.5 | 12.2 |

## 3. Results and discussion

Among the 19 spectra collected from different zeolites, the IR spectra of selected zeolites (Na-ZSM-5, Na-Beta, Na-mordenite, Na-EMC-2, K-L and Na-X) with a broad range of SAR are shown in Fig. 1. As seen, each zeolite has a specific fingerprint associated with the secondary building units of framework structures in the range of 400-820 cm$^{-1}$ [28]. The band at around 950-1090 cm$^{-1}$ is due to the asymmetric stretching mode of Si–O–T(T = Si or Al) [29]. This band is very sensitive and shifts with a change of the SAR of zeolites (Fig. 1). In order to prove that, the SAR of these samples are quantitatively measured with ICP-OES spectroscopy and the correlation between the SAR and the position of this IR band (950–1090 cm$^{-1}$) absorbed at the minimum transmittance is plotted (Fig. 1b). It can be seen that the SAR values correlate linearly to the corresponding wavenumbers with an overall regression coefficient R = 0.9993. The correlation dramatically fluctuates when the SAR ratio exceeds 5 because the shape of this IR band tends to deform when more Al atoms are substituted

by Si atoms. As a result, the IR band is over- lapping with another IR band corresponding to T—O stretching mode at around 1100 $cm^{-1}$ [30]. Thus, the linear equation of $y = 0.0458x - 43.584$, where $y$ is the SAR and $x$ is the asymmetric stretching frequency of the Si—O-T band (in $cm^{-1}$), can be used to determine the SAR value in medium-to-high Al content zeolites ($1 < SAR < 5$).

The occurrence of IR band shifting at 950-1090 $cm^{-1}$ is associated to the vibration, length and angle of Si—O—T bond in zeolites where different distribution of Si and Al atoms in the framework structures also affects the chemical environment of Si. Furthermore, Si MAS NMR spectroscopy was used for validation of the above correlation. For the six samples (Na-ZSM-5, Na-Beta, Na-mordenite, Na-EMC-2, K-L and Na-X), the distribution of $Q_n$ units are shown in the $^{29}Si$ MAS NMR spectra and the SAR values are calculated after deconvolution of the spectra (Fig. 2a). Interestingly, the SAR values for the zeolites with the SAR less than 5 determined by IR and $^{29}Si$ MAS NMR are relatively close, thus showing the good correlation among ICP-OES, IR and NMR spectroscopy methods (Fig. 2b).

It should be mentioned here that the IR and $^{29}Si$ NMR spectroscopies measure the SAR of zeolite frameworks. Hence, it is also important to use other techniques, such as XRF and ICP-OES spectroscopies, that measure the total SAR of zeolites that includes the extra-framework species (if present). Thus, the accuracy of IR spectroscopy method is exemplified in other types of zeolites having SAR values containing medium-to-high Al content ($1 < SAR < 5$) and validated using conventional XRF and ICP-OES spectroscopy techniques. As seen in Table 2, the values estimated using IR method are nearly close to those measured with XRF and ICP-OES spectroscopy methods except the SAR value for zeolite A. The results in Table 2 are further applied and interpreted in the linear regression analysis excluding zeolite A sample (Fig. 3). Interestingly, the correlation coefficient for IR spectroscopy against ICP- OES spectroscopy methods (the most sensitive analytical tool) is found to be satisfactory ($R$ values = 0.967) with considerably low scattering of data points for SAR in the range tested. On the other hand, the linear regression model between IR and XRF spectroscopy methods works reasonably acceptable with $R$ values = 0.975. Hence, this study presents a fast and simple technique complementary to the conventional ICP-OES, XRF and $^{29}Si$ MAS NMR spectroscopy for determination of the SAR ratio in zeolites.

## CRediT authorship contribution statement

**Yik-Ken Ma:** Writing - original draft, Synthesis, Formal analysis, Data interpretation. **Severinne Rigolet:** Formal analysis, Data inter- pretation. **Laure Michelin:** Formal analysis. **Jean-Louis Paillaud:** Synthesis. **Svetlana Mintova:** Formal analysis, Writing - review & editing. **Fitri Khoerunnisa:** Synthesis. **T. Jean Daou:** Synthesis, Formal analysis, Data interpretation, Writing - review & editing. **Eng-Poh Ng:** Supervision, Data interpretation, Writing - review & editing, Project administration.

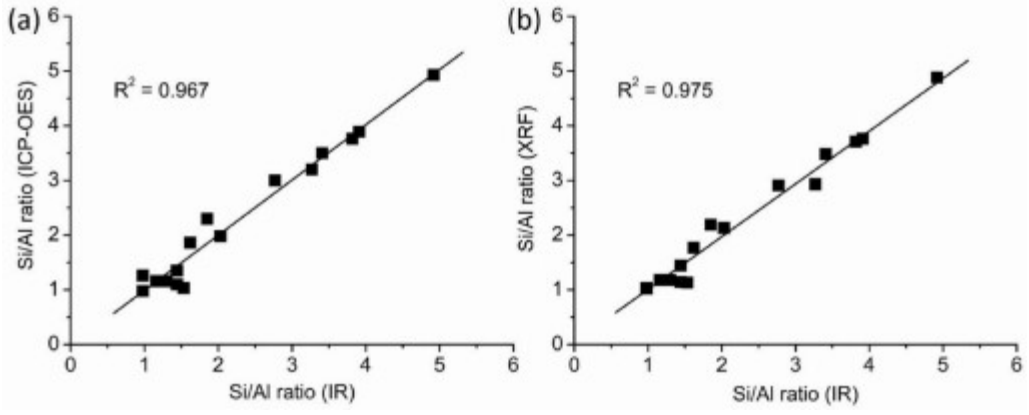


**Fig. 3.** IR regression linearity assessment of SAR validated by (a) ICP-OES and (b) XRF spectroscopy techniques for 16 types of zeolite (K-F, Cs-ABW, Na-EMT, K-W, K-L, K-J, Na-Mordenite, Na-X, Na-Y, Na-EMC-2, hydroxysodalite, heulandite, brewsterite, Na-LSX, offretite and Na-P).

## Declaration of competing interest

The authors declare that they have no known competing financial interests or personal relationships that could have appeared to influence the work reported in this paper.

## Acknowledgement

The financial support from RUI (1001/PKIMIA/8011128) and Institut Universitaire de France grants is gratefully acknowledged. Y.-K. Ma would also like to thank the Graduate Student Financial Assistance (Gra-ASSIST) for the scholarship provided.

## Appendix A. Supplementary data

Supplementary data to this article can be found online at https://doi. org/10.1016/j.micromeso.2020.110683.

## References


[1] I. Deroche, T.J. Daou, C. Picard, B. Coasne, Nat. Commun. 10 (2019) 1 – 10.

[2] G. Majano, E.-P. Ng, L. Lakiss, S. Mintova, Green Chem. 13 (2011) 2435 – 2440.

[3] S.-F. Wong, K. Deekomwong, J. Wittayakun, T.C. Ling, O. Muraza, F. Adam, E.-P. Ng, Mater. Chem. Phys. 196 (2017) 295 – 301.

[4] A. Palcic, V. Valtchev, Appl. Catal. A: Gen. 606 (2020) 117795.

[5] C. Keawkumay, W. Rongchapo, N. Sosaa, S. Suthirakun, I.Z. Koleva, H.A. Aleksandrov, G.N. Vayssilov, J. Wittayakun, Mater. Chem. Phys. 238 (2019) 121824.

[6] E.M. Flanigen, H. Khatami, H.A. Szymanski, in: E.M. Flanigen, L.B. Sand, Advances in Chemistry (Eds.), Molecular Sieve Zeolites-I vol. 101, American Chemical Society, Washington, 1974, pp. 201 – 229 (Chapter 16).

[7] R. Osuga, T. Yokoi, J.N. Kondo, Microporous Mesoporous Mater. 305 (2020) 110345.

[8] U. Lohse, I. Pitsch, E. Schreier, B. Parlitz, K.-H. Schnabel, Appl. Catal. Gen. 129 (1995) 189 – 202.

[9] W. Mozgawa, M. Krol, K. Barczyk, Chemik 65 (2011) 667 – 674.

[10] T.M.A. Ghrear, S. Rigolet, T.J. Daou, S. Mintova, T.C. Ling, S.H. Tan, E.-P. Ng, Microporous Mesoporous Mater. 277 (2019) 78 – 83.

[11] N.H. Ahmad, T.J. Daou, P. Maireles-Torres, M. Zaarour, S. Mintova, T.-C. Ling, E.- P. Ng, Mater. Chem. Phys. 244 (2020) 122688.

[12] S.-F. Wong, H. Awala, A. Vincente, R. Retoux, T.C. Ling, S. Mintova, R.R. Mukti, E.- P. Ng, Microporous Mesoporous Mater. 249 (2017) 105 – 110.

[13] IZA-SC Database of zeolite synthesis. http://www.iza-online.org/synthesis/Recipes /EMC-2.html.

[14] Y.-W. Cheong, K.-L. Wong, T.C. Ling, E.-P. Ng, Mater. Exp. 8 (2018) 463 – 468.

[15] E.-P. Ng, G.K. Lim, G.-L. Khoo, K.-H. Tan, B.S. Ooi, F. Adam, T.C. Ling, K.L. Wong, Mater. Chem. Phys. 155 (2015) 30 – 35.

[16] G.J. Kim, W.S. Ahn, Zeolites 11 (1991) 745 – 750.

[17] E.-P. Ng, L. Delmotte, S. Mintova, ChemSusChem 2 (2009) 255 – 260.

[18] M.-Y. Choo, J.C. Juan, L.E. Oi, T.C. Ling, E.-P. Ng, A.R. Noorsaadah, G. Centi, K. T. Lee, Catal. Sci. Technol. 9 (2019) 772 – 782.

[19] E.-P. Ng, D. Chateigner, T. Bein, V. Valtchev, S. Mintova, Science 335 (2012) 70 – 73.

[20] E.-P. Ng, J.-H. Chow, R.R. Mukti, O. Muraza, T.C. Ling, K.-L. Wong, Mater. Chem. Phys. 201 (2017) 78 – 85.

[21] G.H. Kühl, Zeolites 7 (1987) 451 – 457.

[22] A. Cichocki, P. Koscielniak, Microporous Mesoporous Mater. 29 (1999) 369 – 382.

[23] L.V.C. Rees, S. Chandrasekhar, Zeolites 13 (1993) 535 – 541.

[24] A. Astafan, M.A. Benghalem, Y. Pouilloux, J. Patarin, N. Bats, C. Bouchy, T.J. Daou, L. Pinard, J. Catal. 336 (2016) 1 – 10.

[25] T. Crémoux, I. Batonneau-Gener, A. Moissette, J.-L. Paillaud, M. Hureau, E. Ligner, C. Morais, S. Laforge, C. Marichal, H. Nouali, Phys. Chem. Chem. Phys. 21 (2019) 14892.

[26] E.-P. Ng, H. Awala, J.-P. Ghoy, A. Vicente, T.C. Ling, Y.H. Ng, S. Mintova, F. Adam, Mater. Chem. Phys. 159 (2015) 38 – 45.

[27] G. Engelhardt, U. Lohse, V. Patzelova', M. M"agi, E. Lippmaa, Zeolites 3 (1983) 233 – 238.

[28] C.A.R. Reyesa, C. Williams, O.M.C. Alarcon, Mater. Res. 16 (2013) 424 – 438.

[29] B. Herreros, J. Klinowski, J. Chem. Soc., Faraday Trans. 91 (1995) 1147 – 1154.

[30] K. Byrappa, B.V.S. Kumar, Asian J. Chem. 19 (2007) 4933 – 4935.